Peridynamics: a nonlocal continuum theory

Etienne Emmrich[1], Richard B. Lehoucq[2], and Dimitri Puhst[1]

[1] TU Berlin, Institut für Mathematik, Straße des 17. Juni 136, 10623 Berlin, Germany
emmrich@math.tu-berlin.de, puhst@math.tu-berlin.de

[2] Multiphysics Simulation Technologies, Sandia National Laboratories Albuquerque, NM 87185, USA. Sandia is a multiprogram laboratory operated by Sandia Corporation, a Lockheed Martin Company, for the U.S. Department of Energy under contract DE-AC04-94AL85000.
rblehou@sandia.gov

Summary. The peridynamic theory is a nonlocal theory of continuum mechanics based on an integro-differential equation without spatial derivatives, which can be easily applied in the vicinity of cracks, where discontinuities in the displacement field occur. In this paper we give a survey on important analytical and numerical results and applications of the peridynamic theory.

Key words: peridynamics, nonlocal model, continuum mechanics

1 Introduction

Peridynamics is a nonlocal theory in continuum mechanics. Typically, linear elastic behaviour of solids is well described by the partial differential equation

$$\begin{aligned} &\rho(\boldsymbol{x})\partial_t^2\boldsymbol{u}(\boldsymbol{x},t) = (L\boldsymbol{u})(\boldsymbol{x},t) + \boldsymbol{b}(\boldsymbol{x},t)\,, \quad (\boldsymbol{x},t) \in \Omega \times (0,T)\,, \\ &\text{with } (L\boldsymbol{u})(\boldsymbol{x},t) := (\lambda+\mu)\operatorname{grad}\operatorname{div}\boldsymbol{u}(\boldsymbol{x},t) + \mu \operatorname{div}\operatorname{grad}\boldsymbol{u}(\boldsymbol{x},t)\,, \end{aligned} \tag{1}$$

which is derived from Newton's second law *Force = Mass × Acceleration*. In (1) ρ describes the density of the body; the right-hand side consists of the external force density $\boldsymbol{b}$ as well as inner tensions and macroscopic forces with Lamé parameters λ and μ. The variable $\boldsymbol{u} : \bar{\Omega} \times [0,T] \to \mathbb{R}^d$ with $\Omega \subset \mathbb{R}^d$ and $d \in \{1,2,3\}$ is the displacement field. The limitation of the elastic model (1) is the implicit assumption that the deformation is twice continuously differentiable, which manifests in the inability to model spontaneous cracks and fractures. These are discontinuities of the displacement field and thus, (1) is not defined on cracks or fractures.

In 2000, Silling [41] proposed the peridynamic continuum theory that makes minimal regularity assumptions on the deformation. Instead of spatial

differential operators, integration over differences of the displacement field is used to describe the existing, possibly nonlinear, forces between particles of the solid body. The resulting derivative-free nonlocal peridynamic equation of motion reads

$$\begin{aligned}&\rho(\boldsymbol{x})\partial_t^2\boldsymbol{u}(\boldsymbol{x},t)\\&=\int_{\mathcal{H}(\boldsymbol{x})}\boldsymbol{f}(\boldsymbol{x},\hat{\boldsymbol{x}},\boldsymbol{u}(\boldsymbol{x},t),\boldsymbol{u}(\hat{\boldsymbol{x}},t),t)d\hat{\boldsymbol{x}}+\boldsymbol{b}(\boldsymbol{x},t),\ (\boldsymbol{x},t)\in\Omega\times(0,T).\end{aligned}\tag{2}$$

This theory is named after the greek words *peri* (near) and *dynamis* (force), because in (2) for every particle $\boldsymbol{x}$ the force exerted by each surrounding particle $\hat{\boldsymbol{x}}$ on $\boldsymbol{x}$ is included. The integration domain $\mathcal{H}(\boldsymbol{x})$ describes the volume of particles interacting and is typically the open ball of radius δ surrounding $\boldsymbol{x}$ intersected with Ω. Then δ is called peridynamic horizon. Beyond this horizon we have

$$\boldsymbol{f}(\boldsymbol{x},\hat{\boldsymbol{x}},\boldsymbol{u}(\boldsymbol{x},t),\boldsymbol{u}(\hat{\boldsymbol{x}},t),t)=0,\quad\hat{\boldsymbol{x}}\notin\mathcal{H}(\boldsymbol{x}).\tag{3}$$

The reader is referred to the recent survey Silling & Lehoucq [46] emphasizing the mechanical aspects of the peridynamic continuum theory. This includes proposing the peridynamic balance of energy and thermodynamic restrictions so that the second law of thermodynamics is not violated. The principles of classical statistical mechanics are used to derive the energy and momentum balance laws in Lehoucq & Sears [34]. The aim of this contribution is to give a survey on important analytical and numerical results and applications of this nonlocal continuum theory.

Nonlocal theories taking into account effects of long-range interaction in elastic materials and their application to problems of solid and fracture mechanics have been studied, cf. the pioneering work by Kröner [32], Eringen [28] and the references cited therein, the monographs by Kunin [33] and Rogula [39], and more recently (without being exhaustive) Altan [5, 6], Bažant & Jirásek [9], Chen et al. [16, 15], Lei et al. [35], Pisano & Fuschi [36], Polizzotto [37, 38], Wang & Dhaliwal [48, 47]. In contrast to the peridynamic theory, all these theories rely on spatial derivatives.

This paper is organized as follows. In Section 2 we describe the peridynamic model. First, the bond-based model is demonstrated, where the focus lies on the pairwise force function $\boldsymbol{f}$. Then we derive the linearized model by linearizing the pairwise force function. Afterwards, we describe the state-based peridynamic model, which is a generalization of the bond-based model. Finally in Section 2, other nonlocal models in elasticity are presented.

In Section 3 a survey on the mathematical analysis of the linear bond-based model, the nonlinear bond-based model and state-based model is given. In addition, a nonlocal vector calculus is presented, which is a useful tool for describing the state-based model.

In Section 4 peridynamics is studied as a multiscale method. First, results on the limit of vanishing nonlocality are stated, that is the limit of (2) as the

peridynamic horizon δ goes to zero. Then the modeling of composite materials including the use of two-scale convergence is considered.

Section 5 deals with the numerical approximation of peridynamics by the quadrature formula method.

Finally in Section 6 a few notes on applications and numerical simulations are given.

2 Peridynamic model

2.1 Bond-based model

Since there are no spatial derivatives, boundary conditions are not needed in general for the partial integro-differential equation (2) (although this depends on the singularity behaviour of the integral kernel and the functional analytic setting). Nevertheless, "boundary" conditions can be imposed by prescribing $\boldsymbol{u}$ in a strip along the boundary constraining the solution along a nonzero volume. Hence, (2) is complemented with the initial data

$$\boldsymbol{u}(\cdot,0) = \boldsymbol{u_0} \quad \text{and} \quad \partial_t \boldsymbol{u}(\cdot,0) = \dot{\boldsymbol{u}}_0\,. \tag{4}$$

The interaction between particles within the given horizon is called bond. Since bonds are defined pairwise, this results in a Poisson ratio of $\nu = 1/4$. Thus, due to the relationship $\lambda = 2\mu\nu/(1-2\nu)$, the Lamé parameters λ and μ are identical in the bond-based peridynamic theory.

In the following we will use the notation

$$\boldsymbol{\xi} = \hat{\boldsymbol{x}} - \boldsymbol{x}, \quad \boldsymbol{\eta} = \boldsymbol{u}(\hat{\boldsymbol{x}},t) - \boldsymbol{u}(\boldsymbol{x},t).$$

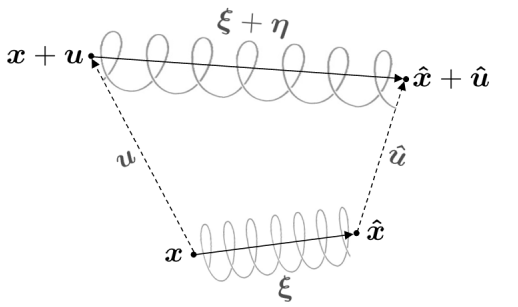

Figure 1. Notation for bond-based model

Note that $\boldsymbol{\xi} + \boldsymbol{\eta}$ is the relative position of the deformed configuration (see Figure 1). Assuming invariance under rigid body motion and no explicit dependence of time, the pairwise force function reads

$$\boldsymbol{f}(\boldsymbol{x},\hat{\boldsymbol{x}},\boldsymbol{u}(\boldsymbol{x},t),\boldsymbol{u}(\hat{\boldsymbol{x}},t),t)=\boldsymbol{f}(\boldsymbol{x},\hat{\boldsymbol{x}},\boldsymbol{\eta}).$$

Combining Newton's third law *actio et reactio*, which gives

$$\boldsymbol{f}(\hat{\boldsymbol{x}},\boldsymbol{x},-\boldsymbol{\eta})=-\boldsymbol{f}(\boldsymbol{x},\hat{\boldsymbol{x}},\boldsymbol{\eta}), \tag{5}$$

with the balance of angular momentum leads to the conclusion that the pairwise force function is parallel to $\boldsymbol{\xi}+\boldsymbol{\eta}$. We call $\boldsymbol{f}$ homogenous, if

$$\boldsymbol{f}(\boldsymbol{x},\hat{\boldsymbol{x}},\boldsymbol{\eta})=\boldsymbol{f}(\boldsymbol{\xi},\boldsymbol{\eta})$$

is fulfilled for all $\boldsymbol{\xi}$ and $\boldsymbol{\eta}$.[3] Furthermore, a material is called microelastic if there exists a so-called pairwise micropotential w such that $\boldsymbol{f}(\boldsymbol{\xi},\boldsymbol{\eta})=\nabla_{\boldsymbol{\eta}}w(\boldsymbol{\xi},\boldsymbol{\eta})$. One of the simplest nonlinear models that has been suggested is the proportional microelastic material model with

$$\boldsymbol{f}(\boldsymbol{\xi},\boldsymbol{\eta})=c_{d,\delta}\,s(\boldsymbol{\xi},\boldsymbol{\eta})\,\frac{\boldsymbol{\xi}+\boldsymbol{\eta}}{|\boldsymbol{\xi}+\boldsymbol{\eta}|}\chi_{(0,\delta)}(|\boldsymbol{\xi}|), \tag{6}$$

where

$$s(\boldsymbol{\xi},\boldsymbol{\eta})=\frac{|\boldsymbol{\xi}+\boldsymbol{\eta}|-|\boldsymbol{\xi}|}{|\boldsymbol{\xi}|}$$

denotes the bond stretch[4] that is the relative change of the length of a bond. By $|\cdot|$ we denote the Euclidean norm. In this case the related micropotential is given by

$$w(\boldsymbol{\xi},\boldsymbol{\eta})=\frac{c_{d,\delta}s^2(\boldsymbol{\xi},\boldsymbol{\eta})}{2}\,|\boldsymbol{\xi}|\,\chi_{(0,\delta)}(|\boldsymbol{\xi}|),$$

where we have chosen the micropotential such that $w(\boldsymbol{\xi},\boldsymbol{0})=0$. The constants of proportionality are

$$c_{1,\delta}=\frac{18K}{5\delta^2},\ c_{2,\delta}=\frac{72K}{5\pi\delta^3},\ c_{3,\delta}=\frac{18K}{\pi\delta^4}$$

with the bulk modulus $K=\lambda(1+\nu)/(3\nu)=5\lambda/3$.

Let the kinetic and elastic energy density be defined as

$$\begin{aligned}e_{kin}(\boldsymbol{x},t)&=\frac{1}{2}\rho(\boldsymbol{x})\,|\partial_t\boldsymbol{u}(\boldsymbol{x},t)|^2\ ,\\ e_{el}(\boldsymbol{x},t)&=\frac{1}{2}\int_{\mathcal{H}(\boldsymbol{x})}w(\hat{\boldsymbol{x}}-\boldsymbol{x},\boldsymbol{u}(\hat{\boldsymbol{x}},t)-\boldsymbol{u}(\boldsymbol{x},t))d\hat{\boldsymbol{x}}\,,\end{aligned}$$

and let $l=e_{kin}-e_{el}-e_{ext}$ denote the total energy density with $e_{ext}(\boldsymbol{x},t)=-\boldsymbol{b}(\boldsymbol{x},t)\cdot\boldsymbol{u}(\boldsymbol{x},t)$ induced by the external force density $\boldsymbol{b}$. Then equation (2) can be derived from the variational problem of minimizing the functional

[3] Note that the notation $\boldsymbol{f}=\boldsymbol{f}(\boldsymbol{\xi},\boldsymbol{\eta})$ is somewhat ambigious. Indeed, for a given function $\boldsymbol{u}=\boldsymbol{u}(\boldsymbol{x},t)$ the mathematical correct way to describe $\boldsymbol{f}$ is using the Nemytskii operator $F:\boldsymbol{u}\mapsto F\boldsymbol{u}$ with $(F\boldsymbol{u})(\boldsymbol{x},\hat{\boldsymbol{x}},t)=\boldsymbol{f}(\hat{\boldsymbol{x}}-\boldsymbol{x},\boldsymbol{u}(\hat{\boldsymbol{x}},t)-\boldsymbol{u}(\boldsymbol{x},t))$.

[4] For the notation $s=s(\boldsymbol{\xi},\boldsymbol{\eta})$, see also Footnote 3.

$$\boldsymbol{u} \mapsto \int_0^T \int_\Omega l(\boldsymbol{x}, t) d\boldsymbol{x} dt,$$

see also Emmrich & Weckner [26].

In order to model cracks and simulate fracture, bonds are allowed to break. This is realized by multiplying the pairwise force function, given, e.g., by (6), the function

$$\mu(\boldsymbol{\xi}, \boldsymbol{\eta}, t) = \begin{cases} 1 & \text{if } s(\boldsymbol{\xi}, \boldsymbol{u}(\hat{\boldsymbol{x}}, \tau) - \boldsymbol{u}(\boldsymbol{x}, \tau)) \leq s_0 \ \forall \tau \leq t \\ 0 & \text{otherwise} \end{cases}$$

for some critical bond stretch s_0 for breakage. Note that the resulting pairwise force function now explicitly depends on time t.

2.2 Linearization

A first-order approximation justifies for small relative displacements $\boldsymbol{\eta}$ the general linear ansatz

$$\boldsymbol{f}(\boldsymbol{\xi}, \boldsymbol{\eta}) = \boldsymbol{f}_0(\boldsymbol{\xi}) + \boldsymbol{C}(\boldsymbol{\xi})\boldsymbol{\eta}$$

with the stiffness tensor (or micromodulus function) $\boldsymbol{C} = \boldsymbol{C}(\boldsymbol{\xi})$ and $\boldsymbol{f}_0$ denoting forces in the reference configuration. Without loss of generality, we may assume $\boldsymbol{f}_0 \equiv 0$ since otherwise $\boldsymbol{f}_0$ can be incorporated into the right-hand side $\boldsymbol{b}$. In general the stiffness tensor $\boldsymbol{C}$ is not definite. However, $\boldsymbol{C}$ has to be symmetric with respect to its argument as well as with respect to its tensor structure such that $\boldsymbol{C}(\boldsymbol{\xi}) = \boldsymbol{C}(-\boldsymbol{\xi})$ and $\boldsymbol{C}(\boldsymbol{\xi})^T = \boldsymbol{C}(\boldsymbol{\xi})$. The corresponding micropotential is then given by $w(\boldsymbol{\xi}, \boldsymbol{\eta}) = \boldsymbol{\eta}^T \boldsymbol{C}(\boldsymbol{\xi})\boldsymbol{\eta}/2$. In view of (3) we shall require $\boldsymbol{C}(\boldsymbol{\xi}) = 0$ if $|\boldsymbol{\xi}| \geq \delta$.

The stiffness tensor can be shown to read as

$$\boldsymbol{C}(\boldsymbol{\xi}) = \lambda_{d,\delta}(|\boldsymbol{\xi}|)\boldsymbol{\xi} \otimes \boldsymbol{\xi}$$

for a linear microelastic material (see also Silling [41]), where $\otimes$ denotes the dyadic product. The function $\lambda_{d,\delta} : \mathbb{R}_0^+ \to \mathbb{R}$ with $\lambda_{d,\delta}(r) = 0$ for $r \geq \delta$ determines the specific material model and depends on the dimension d and the peridynamic horizon δ. The linear peridynamic equation of motion (2) now reads as

$$\rho(\boldsymbol{x})\partial_t^2 \boldsymbol{u}(\boldsymbol{x}, t) = (L_{d,\delta}\boldsymbol{u})(\boldsymbol{x}, t) + \boldsymbol{b}(\boldsymbol{x}, t)\,, \quad (\boldsymbol{x}, t) \in \Omega \times (0, T)\,,$$

with

$$(L_{d,\delta}\boldsymbol{u})(\boldsymbol{x}, t) := \int_{\mathcal{H}(\boldsymbol{x})} \boldsymbol{\lambda}_{d,\delta}(|\hat{\boldsymbol{x}} - \boldsymbol{x}|)(\hat{\boldsymbol{x}} - \boldsymbol{x}) \otimes (\hat{\boldsymbol{x}} - \boldsymbol{x}) \cdot (\boldsymbol{u}(\hat{\boldsymbol{x}}, t) - \boldsymbol{u}(\boldsymbol{x}, t)) d\hat{\boldsymbol{x}} \tag{7}$$

The recent report Du et al. [20] also demonstrates how the one-dimensional equation (7) can be written as two first-order in time nonlocal advection equations. Note that $\lambda_{d,\delta}$ can have a singularity at $r = 0$. The standard example is

the linearization of (6) with $\lambda_{d,\delta}(r) = c_{d,\delta} r^{-3} \chi_{(0,\delta)}(r)$. Unfortunately, in this model, the interaction jumps to zero if $r = \delta$. This jump discontinuity can be avoided by taking $\lambda_{d,\delta}(r) = \tilde{c}_{d,\delta} r^{-3} \exp(-\delta^2/(\delta^2 - r^2)) \chi_{(0,\delta)}(r)$ with a suitable constant of proportionality $\tilde{c}_{d,\delta}$, see also Emmrich & Weckner [25]. This is of advantage also for the numerical approximation relying on quadrature.

2.3 State-based model

The integral

$$\int_{\mathcal{H}(\boldsymbol{x})} \boldsymbol{f}\big(\hat{\boldsymbol{x}} - \boldsymbol{x}, \boldsymbol{u}(\hat{\boldsymbol{x}}, t) - \boldsymbol{u}(\boldsymbol{x}, t)\big)\, d\hat{\boldsymbol{x}}$$

expresses that the internal force density at $\hat{\boldsymbol{x}}$ is a summation of forces over all vectors $\hat{\boldsymbol{x}} - \boldsymbol{x}$. Moreover, the summands are independent from each other. As demonstrated by Silling [41, §11], this effectively limits Poisson's ratio to a value of one-fourth for homogenous deformations of linear isotropic solids. In the same paper, a generalization is presented that augments the above integral with the term

$$e\big(\vartheta(\boldsymbol{x})\big)\,, \text{ where } \vartheta(\boldsymbol{x}) = \int j\big(|\hat{\boldsymbol{x}} - \boldsymbol{x}|\big) |\hat{\boldsymbol{x}} - \boldsymbol{x} + \boldsymbol{u}(\hat{\boldsymbol{x}}, t) - \boldsymbol{u}(\boldsymbol{x}, t)|\, d\hat{\boldsymbol{x}}.$$

The quantity ϑ is a weighted average of all the bonds $\hat{\boldsymbol{x}} - \boldsymbol{x} + \boldsymbol{u}(\hat{\boldsymbol{x}}, t) - \boldsymbol{u}(\boldsymbol{x}, t)$ and provides the volume of a deformed sphere that is centered at $\boldsymbol{x}$ in the reference configuration; the quantity e then acts as a volume-dependent strain energy term that incorporates the collective motion of all the $\hat{\boldsymbol{x}} - \boldsymbol{x}$ simultaneously. The linearized operator is then shown to circumvent the restriction of Poisson's ratio to a value of one-fourth to its allowable values. The recent report Seleson, Parks & Gunzburger [40] demonstrates a symbiotic relationship between this generalization and an embedded atom (EAM) molecular dynamic potential.

Silling et al. [44] introduces the peridynamic state theory, a subsequent generalization to the approach in Silling [41, §15]. The integral in (2) is replaced by $L_{\mathrm{PD}}\boldsymbol{u}$ where

$$(L_{\mathrm{PD}}\boldsymbol{u})(\boldsymbol{x}, t) = \int_{\mathcal{H}(\boldsymbol{x})} \Big(\underline{\mathbf{T}}[\boldsymbol{x}, t]\langle \hat{\boldsymbol{x}} - \boldsymbol{x}\rangle - \underline{\mathbf{T}}[\hat{\boldsymbol{x}}, t]\langle \boldsymbol{x} - \hat{\boldsymbol{x}}\rangle\Big)\, d\hat{\boldsymbol{x}} \tag{8}$$

leading to the equation of motion

$$\rho(\boldsymbol{x})\partial_t^2 \boldsymbol{u}(\boldsymbol{x}, t) = (L_{\mathrm{PD}}\boldsymbol{u})(\boldsymbol{x}, t) + \boldsymbol{b}(\boldsymbol{x}, t),\ (\boldsymbol{x}, t) \in \Omega \times (0, T). \tag{9}$$

The term $L_{\mathrm{PD}}\boldsymbol{u}$ is a functional of displacement representing the internal force density (per unit volume) that is exerted upon $\boldsymbol{x}$ by other points in the body. The *force state* $\underline{\mathbf{T}}[\boldsymbol{x}, t]$ at $\boldsymbol{x}$ at time t is a mapping from the bond $\hat{\boldsymbol{x}} - \boldsymbol{x}$ to a force density (per unit volume) at $\boldsymbol{x}$ and is assumed to be zero outside the horizon δ. A material model is therefore provided by a relation between the deformation near $\boldsymbol{x}$ and the force state at $\boldsymbol{x}$, e.g.,

$$\underline{\mathbf{T}} = \underline{\mathbf{T}}(\underline{\mathbf{Y}}) \tag{10}$$

where $\underline{\mathbf{Y}}$ is the *deformation state*, a mapping from bonds connected to any $\boldsymbol{x}$ to the deformed images of these bonds, e.g.,

$$\underline{\mathbf{Y}}[\boldsymbol{x},t]\langle\hat{\boldsymbol{x}}-\boldsymbol{x}\rangle = \hat{\boldsymbol{x}}-\boldsymbol{x}+\boldsymbol{u}(\hat{\boldsymbol{x}},t)-\boldsymbol{u}(\boldsymbol{x},t). \tag{11}$$

Although the deformation or force state maps vectors into vectors, they are more complex than second order tensors because the mapping may be nonlinear and even discontinuous. The constitutive relation (10) explains that the force state maps the collective motion about $\boldsymbol{x}$ in contrast to the relation $f(\hat{\boldsymbol{x}}-\boldsymbol{x},\boldsymbol{u}(\hat{\boldsymbol{x}},t)-\boldsymbol{u}(\boldsymbol{x},t))$. A bond-based force is recovered via the identification $\underline{\mathbf{T}}[\boldsymbol{x},t]\langle\hat{\boldsymbol{x}}-\boldsymbol{x}\rangle = 1/2 f\big(\hat{\boldsymbol{x}}-\boldsymbol{x},\boldsymbol{u}(\hat{\boldsymbol{x}},t)-\boldsymbol{u}(\boldsymbol{x},t)\big)$ because then

$$\begin{aligned}\underline{\mathbf{T}}[\boldsymbol{x},t]\langle\hat{\boldsymbol{x}}-\boldsymbol{x}\rangle &- \underline{\mathbf{T}}[\hat{\boldsymbol{x}},t]\langle\boldsymbol{x}-\hat{\boldsymbol{x}}\rangle \\ &= \frac{1}{2}f\big(\hat{\boldsymbol{x}}-\boldsymbol{x},\boldsymbol{u}(\hat{\boldsymbol{x}},t)-\boldsymbol{u}(\boldsymbol{x},t)\big) - \frac{1}{2}f\big(\boldsymbol{x}-\hat{\boldsymbol{x}},\boldsymbol{u}(\boldsymbol{x},t)-\boldsymbol{u}(\hat{\boldsymbol{x}},t)\big) \\ &= f\big(\hat{\boldsymbol{x}}-\boldsymbol{x},\boldsymbol{u}(\hat{\boldsymbol{x}},t)-\boldsymbol{u}(\boldsymbol{x},t)\big)\end{aligned}$$

where we invoked (5) for the last equality. This identification reveals another important distinction between the bond-based and state theories. Namely, that force interaction is carried by the bond in the former theory while the interaction is split between the force state at $\boldsymbol{x}$ and $\hat{\boldsymbol{x}}$ in the latter theory.

The paper [44] introduces a linear peridynamic state material model generalizing the linear bond-based material model. Silling [43] further generalizes the linear peridynamic state material model. A key concept is that of the modulus state, a second order tensor,

$$\underline{\mathbb{K}} = \nabla\underline{\mathbf{T}}\langle\underline{\mathbf{Y}}\rangle\colon \mathbb{R}^3\times\mathbb{R}^3 \to \mathbb{R}^{3\times 3},$$

the Fréchet derivative of the force state with respect to $\underline{\mathbf{Y}}$. The modulus state represents the peridynamic analogue of the fourth order tensor in the classical linear elastic theory and so allows us to linearize a force state about a time-independent deformation state $\underline{\mathbf{Y}}^0$, e.g.,

$$\underline{\mathbf{T}}(\underline{\mathbf{U}})\langle\hat{\boldsymbol{x}}-\boldsymbol{x}\rangle = \underline{\mathbf{T}}(\underline{\mathbf{Y}}^0)\langle\hat{\boldsymbol{x}}-\boldsymbol{x}\rangle + \int_{\mathcal{H}(\boldsymbol{x})} \underline{\mathbb{K}}\langle\hat{\boldsymbol{x}}-\boldsymbol{x},\tilde{\boldsymbol{x}}-\boldsymbol{x}\rangle\underline{\mathbf{U}}\langle\tilde{\boldsymbol{x}}-\boldsymbol{x}\rangle\, d\tilde{\boldsymbol{x}} \tag{12}$$

where $\underline{\mathbf{U}}$ is the displacement state field defined by

$$\underline{\mathbf{U}}[\boldsymbol{x}]\langle\hat{\boldsymbol{x}}-\boldsymbol{x}\rangle = \underline{\mathbf{Y}}^0[\boldsymbol{x}]\langle\hat{\boldsymbol{x}}-\boldsymbol{x}\rangle - (\hat{\boldsymbol{x}}-\boldsymbol{x}). \tag{13}$$

Assume that the body force $\boldsymbol{b}$ has the decomposition $\boldsymbol{b}^0+\hat{\boldsymbol{b}}$ for some time-independent external force density $\boldsymbol{b}^0$ so tat

$$\int_{\mathcal{H}(\boldsymbol{x})} \Big(\underline{\mathbf{T}}^0[\boldsymbol{x}]\langle\hat{\boldsymbol{x}}-\boldsymbol{x}\rangle - \underline{\mathbf{T}}^0[\hat{\boldsymbol{x}}]\langle\boldsymbol{x}-\hat{\boldsymbol{x}}\rangle\Big)\, d\hat{\boldsymbol{x}} + \boldsymbol{b}^0(\boldsymbol{x}) = \boldsymbol{0}, \tag{14}$$

where $\underline{\mathbf{T}}^0 \equiv \underline{\mathbf{T}}(\underline{\mathbf{Y}}^0)$. Inserting the linearized force state (12) into the equation of motion (9), and invoking relations (13) and (14) results in an equation of motion with body force $\hat{\boldsymbol{b}}$ and force state given by the integral operator of (12).

An important material model is the *elastic* peridynamic material, defined by

$$\underline{\mathbf{T}}(\underline{\mathbf{Y}}) = \nabla W(\underline{\mathbf{Y}}) \tag{15}$$

where ∇W is the Fréchet derivative of the scalar valued function W, the *strain energy density function*. This elastic material model is the peridynamic analogue of the classical elastic model

$$\boldsymbol{\sigma} = \frac{\partial W}{\partial \boldsymbol{F}},$$

where $\boldsymbol{\sigma}$ and $\boldsymbol{F}$ are the Piola–Kirchoff stress tensor and deformation gradient, respectively. The modulus state is then $\underline{\mathbb{K}} = \nabla\nabla W(\underline{\mathbf{Y}})$. The reader is referred to Silling [43] for example material models.

2.4 Other nonlocal models in elasticity theory

In Section 1, references to various nonlocal models in elasticity are stated. Two examples are given in the following. In [22], Duruk, Erbay and Erkip study the one-dimensional nonlocal nonlinear Cauchy problem

$$\partial_t^2 u(x,t) = \partial_x^2 \int_{\mathbb{R}} \beta(x-\hat{x}) g(u(\hat{x},t)) d\hat{x}\,, \quad (x,t) \in \mathbb{R} \times (0,\infty)\,, \tag{16}$$

complemented with initial conditions. Here β is an integrable kernel function whose Fourier transform satisfies a certain growth condition, and g is some nonlinear function. Global existence and blow-up conditions are investigated. For a so-called double-exponential kernel β equation (16) turns out to be equivalent to the higher-order Boussinesq equation

$$u_{tt} - u_{xx} - a u_{xxtt} + b u_{xxxxtt} = (g(u))_{xx}$$

with positive constants a, b. This example illustrates that, first, nonlocal models so far still depend on spatial derivatives and, second, nonlocal models may be related with local models described by partial differential equations with higher-order spatial derivatives.

In Eringen [28] and Polizzotto [37] the Eringen model is proposed and developed. Combining the equation of motion

$$\rho(x)\boldsymbol{u}_{tt}(\boldsymbol{x},t) = \operatorname{div} \boldsymbol{\sigma}(\boldsymbol{u}(\boldsymbol{x},t)) + \boldsymbol{b}(\boldsymbol{x},t)$$

with a nonlocal formulation of the stress tensor

$$\boldsymbol{\sigma}(\boldsymbol{v}(\boldsymbol{x})) = \int_\Omega \alpha(|\hat{\boldsymbol{x}} - \boldsymbol{x}|) \boldsymbol{s}(\boldsymbol{v}(\hat{\boldsymbol{x}})) d\hat{\boldsymbol{x}},$$

which incorporates the entire body Ω with a suitable interaction kernel α and the classical stress $\boldsymbol{s}$ from Hooke's law

$$\boldsymbol{s}(\boldsymbol{v}) = \boldsymbol{S} : \frac{1}{2}\left[\nabla \boldsymbol{v} + (\nabla \boldsymbol{v})^T\right]$$

with stiffness tensor $\boldsymbol{S}$, gives a nonlocal equation of motion in linear elasticity.

3 Mathematical analysis of the peridynamic model

3.1 Linear bond-based model in L^2

First results on existence, uniqueness and qualitative behaviour of solutions to the peridynamic equation of motion have been presented in Emmrich & Weckner [24] for the infinite peridynamic bar. Besides well-posedness in L^∞ also nonlinear dispersion relations as well as jump relations for discontinuous solutions have been studied.

In [23], Emmrich and Weckner have proved results on existence, uniqueness, and continuous dependence of the solution for the linear model with data in an L^p-setting for $p > 2$ if $d = 2$ and $p > 3/2$ if $d = 3$. Moreover, a formal representation of the exact solution and a priori estimates are given. In [25], Emmrich and Weckner proved well-posedness of the linear model in $L^\infty(\Omega)^d$ and in $L^2(\Omega)^d$ under the condition

$$\int_0^\delta |\lambda_{d,\delta}(r)|\, r^{d+1} dr < \infty. \tag{17}$$

Theorem 1. *If (17) is fulfilled, then there exists for every $\boldsymbol{u}_0$, $\dot{\boldsymbol{u}}_0 \in L^2(\Omega)^d$, $\boldsymbol{b} \in L^1(0,T;L^2(\Omega)^d)$ a unique solution $\boldsymbol{u} \in \mathcal{C}^1([0,T],L^2(\Omega)^d)$ to the initial-value problem (7), (4) that satisfies the a priori estimate*

$$\|\boldsymbol{u}\|_{\mathcal{C}^1([0,T],L^2(\Omega)^d)} \le C_{d,\delta}\left(\|\boldsymbol{u}_0\|_{L^2(\Omega)^d} + \|\dot{\boldsymbol{u}}_0\|_{L^2(\Omega)^d} + \|\boldsymbol{b}\|_{L^1(0,T;L^2(\Omega)^d)}\right).$$

If $\boldsymbol{b} \in \mathcal{C}([0,T],L^2(\Omega)^d)$ then $\boldsymbol{u} \in \mathcal{C}^2([0,T],L^2(\Omega)^d)$.

Moreover, other properties of the peridynamic integral operator defined through (7) such as dissipativity and self-adjointness are analyzed in Emmrich & Weckner [25].

In [21, 49] Du and Zhou consider the case $\Omega = \mathbb{R}^d$. Let $\mathcal{M}_\lambda(\mathbb{R}^d)^d$ be the space of functions $\boldsymbol{u} \in L^2(\mathbb{R}^d)^d$ with

$$\int_{\mathbb{R}^d} (\mathcal{F}\boldsymbol{u})(\boldsymbol{y}) \cdot (\boldsymbol{I} + \boldsymbol{M}_\delta(\boldsymbol{y}))(\mathcal{F}\boldsymbol{u}) d\boldsymbol{y} < \infty,$$

depending on $\lambda_{d,\delta}$ since

$$\boldsymbol{M}_\delta(\boldsymbol{y}) = \int_0^\delta \lambda_{d,\delta}(|\hat{\boldsymbol{x}}|)(1-\cos(\boldsymbol{y}\cdot\hat{\boldsymbol{x}}))\hat{\boldsymbol{x}}\otimes\hat{\boldsymbol{x}}d\hat{\boldsymbol{x}}.$$

Here $\mathcal{F}\boldsymbol{u}$ denotes the Fourier transform of $\boldsymbol{u}$.

A natural condition coming from the comparison of the deformation energy density of a homogeneous body under isotropic expansion arising from the peridynamic model with the energy density known from the classical linear elasticity theory is

$$\int_0^\delta \lambda_{d,\delta}(r)r^{d+3}dr < \infty. \tag{18}$$

Theorem 2. *Assume $\lambda_{d,\delta}(r) > 0$ for $0 < r < \delta$, (18) and $\boldsymbol{u}_0 \in \mathcal{M}_\lambda(\mathbb{R}^d)^d$, $\dot{\boldsymbol{u}}_0 \in L^2(\mathbb{R}^d)^d$ and $\boldsymbol{b} \in L^2(0,T;L^2(\mathbb{R}^d)^d)$. Then the initial-value problem (7), (4) has a unique solution $\boldsymbol{u} \in C([0,T],\mathcal{M}_\lambda(\mathbb{R}^d)^d)$ with $\boldsymbol{u}_t \in L^2(0,T;L^2(\mathbb{R}^d)^d)$.*

If in addition condition (17) is valid, then Du and Zhou show that the space $\mathcal{M}_\lambda(\mathbb{R}^d)^d$ is equivalent to the space $L^2(\mathbb{R}^d)^d$.

3.2 Linear bond-based model in H^σ ($\sigma \in (0,1)$)

The solution of Theorem 2 can take values in a fractional Sobolev space. Indeed, if

$$c_1 r^{-2-d-2\sigma} \le \lambda_{d,\delta}(r) \le c_2 r^{-2-d-2\sigma}, \quad \forall\, 0 < r \le \delta \tag{19}$$

for some exponent $\sigma \in (0,1)$ and positive constants c_1 and c_2, then Theorem 2 remains true and the space $\mathcal{M}_\lambda(\mathbb{R}^d)^d$ is equivalent to the fractional Sobolev space $H^\sigma(\mathbb{R}^d)^d$.

Additionally also the stationary problem is investigated in [21, 49].

3.3 Nonlinear bond-based model

A first result towards the nonlinear model is Erbay, Erkip & Muslu [27] analyzing the nonlinear elastic bar. They consider the one-dimensional initial value problem

$$\begin{aligned} &u_{tt} = \int_{\mathbb{R}} \alpha(\hat{x}-x)g(u(\hat{x},t)-u(x,t))d\hat{x}, \quad x\in\mathbb{R},\ t>0,\\ &u(x,0)=u_0, \quad u_t(x,0)=\dot{u}_0, \quad x\in\mathbb{R}. \end{aligned} \tag{20}$$

Applying Banach's fixed point theorem the following theorems are proven.

Theorem 3. *Let $X = C_b(\mathbb{R})$ or let $X = L^p(\mathbb{R}) \cap L^\infty(\mathbb{R})$ with $1 \le p \le \infty$. Assume $\alpha \in L^1(\mathbb{R})$ and $g \in \mathcal{C}^1(\mathbb{R})$ with $g(0) = 0$. Then there exists $T > 0$ such that the Cauchy problem (20) is locally well-posed with solution in $\mathcal{C}^2([0,T],X)$ for initial data $u_0, \dot{u}_0 \in X$.*

Theorem 4. *Let $X = \mathcal{C}_b^1(\mathbb{R})$ or let $X = W^{1,p}(\mathbb{R})$ with $1 \le p \le \infty$. Assume $\alpha \in L^1(\mathbb{R})$ and $g \in \mathcal{C}^2(\mathbb{R})$ with $g(0) = 0$. Then there exists $T > 0$ such that the Cauchy problem (20) is locally well-posed with solution in $\mathcal{C}^2([0,T], X)$ for initial data $u_0, \dot{u}_0 \in X$.*

The authors of [27] remark that the proofs of the above theorems can be easily adapted to the more general peridynamic equation with a nonlinear pairwise force function $f(\xi, \eta)$, where f is continuously differentiable in η for almost every ξ and fulfils additional assumptions. For a more specific type of nonlinearities, Erbay, Erkip & Muslu [27] proved well-posedness in fractional Sobolev spaces.

Theorem 5. *Let $\sigma > 0$ and $u_0, \dot{u}_0 \in W^{\sigma,2}(\mathbb{R}) \cap L^\infty(\mathbb{R})$. Assume $\alpha \in L^1(\mathbb{R})$ and $g(\eta) = \eta^3$. Then there exists $T > 0$ such that the Cauchy problem (20) is locally well-posed with solution in $\mathcal{C}^2([0,T], W^{\sigma,2}(\mathbb{R}) \cap L^\infty(\mathbb{R}))$.*

Furthermore, blow up conditions for these solutions are investigated, which we shall not present here.

3.4 State-based model and nonlocal vector calculus

The recent reports Du et al. [17, 18] consider a nonlocal vector calculus building upon the ideas of Gunzburger & Lehoucq [29]. The nonlocal vector calculus is applied in Du et al. [19] to establish the well-posedness of the linear peridynamic state equilibrium equation. We briefly summarize the vector calculus and well-posedness for the case of a linear isotropic material.

Let Ω denote an open subset of $\mathbb{R}^d$ and let $\boldsymbol{\alpha} = \boldsymbol{\alpha}(\boldsymbol{x}, \boldsymbol{y})$ denote an anti-symmetric mapping, i.e., $\boldsymbol{\alpha}(\boldsymbol{x}, \boldsymbol{y}) = -\boldsymbol{\alpha}(\boldsymbol{y}, \boldsymbol{x})$. Define the nonlocal divergence operator of a tensor $\boldsymbol{\Psi}$ and its adjoint operator,

$$\begin{aligned} \mathcal{D}_t(\boldsymbol{\Psi})(\boldsymbol{x}) &= \int_{\mathbb{R}^d} \big(\boldsymbol{\Psi}(\boldsymbol{x}, \boldsymbol{y}) + \boldsymbol{\Psi}(\boldsymbol{y}, \boldsymbol{x})\big) \cdot \boldsymbol{\alpha}(\boldsymbol{x}, \boldsymbol{y})\, d\boldsymbol{y} \quad \text{for } \boldsymbol{x} \in \Omega, \\ \mathcal{D}_t^*(\boldsymbol{v})(\boldsymbol{x}, \boldsymbol{y}) &= -\big(\boldsymbol{v}(\boldsymbol{y}) - \boldsymbol{v}(\boldsymbol{x})\big) \otimes \boldsymbol{\alpha}(\boldsymbol{x}, \boldsymbol{y}) \quad \text{for } \boldsymbol{x}, \boldsymbol{y} \in \Omega, \end{aligned}$$

established via $\big(\mathcal{D}_t(\boldsymbol{\Psi}), \boldsymbol{v}\big)_\Omega = \big(\boldsymbol{\Psi}, \mathcal{D}_t^*(\boldsymbol{v})\big)_{\Omega\times\Omega}$, inner products on $L^2(\Omega)$ and $L^2(\Omega \times \Omega)$, respectively. The operators $\mathcal{D}_t(\boldsymbol{\Psi})$ and $\mathcal{D}_t^*(\boldsymbol{v})$ return a vector and tensor respectively. Let $\omega = \omega(\boldsymbol{x}, \boldsymbol{y})$ and $\mathbf{U} = \mathbf{U}(\boldsymbol{x})$ denote a nonnegative scalar function and tensor, respectively. The choice $\boldsymbol{\Psi}(\boldsymbol{x}, \boldsymbol{y}) = \omega(\boldsymbol{x}, \boldsymbol{y})\mathbf{U}(\boldsymbol{x})$ results in the *weighted nonlocal divergence operator $\mathcal{D}_{t,\omega}$ for tensors* and its adjoint operator,

$$\begin{aligned} \mathcal{D}_{t,\omega}\big(\mathbf{U}\big)(\boldsymbol{x}) &= \mathcal{D}_t\big(\omega(\boldsymbol{x}, \boldsymbol{y})\mathbf{U}(\boldsymbol{x})\big)(\boldsymbol{x}) \quad \text{for } \boldsymbol{x} \in \Omega, \\ \mathcal{D}_{t,\omega}^*\big(\boldsymbol{u}\big)(\boldsymbol{x}) &= \int_{\mathbb{R}^d} \mathcal{D}_t^*(\boldsymbol{u})(\boldsymbol{x}, \boldsymbol{y})\, \omega(\boldsymbol{x}, \boldsymbol{y})\, d\boldsymbol{y} \quad \text{for } \boldsymbol{x} \in \Omega. \end{aligned}$$

The distinction between $\mathcal{D}_t^*(\boldsymbol{v})$ and $\mathcal{D}_{t,\omega}^*\big(\boldsymbol{u}\big)$ is that the former is a tensor on $\Omega \times \Omega$ while the latter is a tensor on Ω.

In the case of a linear peridynamic solid, define the operator

$$\mathcal{L}(\boldsymbol{u}) = \mathcal{D}_t\big(\eta\big(\mathcal{D}_t^*(\boldsymbol{u})\big)^T\big) + \mathcal{D}_{t,w}\big(\gamma \mathrm{Tr}\big(\mathcal{D}_{t,\omega}^*(\boldsymbol{u})\big)\mathrm{I}\big) \tag{21}$$

where η and γ are materials constants. Mild conditions may also be supplied so that

$$\mathcal{L} \to L \equiv (\lambda + \mu)\,\mathrm{grad}\,\mathrm{div} + \mu\,\mathrm{div}\,\mathrm{grad}$$

in $H^{-1}(\mathbb{R}^d)$ as the horizon decreases. Here, μ and λ are the Lamé parameters that are given as expressions in terms of η and γ. The first term on the right-hand side of (21) corresponds to the bond-based material model and is the peridynamic analogue of $\mu\,\mathrm{div}\,\mathrm{grad} + \mu\,\mathrm{grad}\,\mathrm{div}$. The second term on the right-hand side of (21) accounts for volumetric terms associated with Poisson ratio not equal to one fourth and is the peridynamic analogue of $\lambda\,\mathrm{grad}\,\mathrm{div}$.

In words, the peridynamic operator $\mathcal{L}$ converges to the Navier operator as the horizon tends to zero where the horizon is given by the support of $\boldsymbol{\alpha}\cdot\boldsymbol{\alpha}$ and ω in the two operators in the right-hand side of (21). In contrast to the Navier operator, the peridynamic operator $\mathcal{L}$ only depends upon spatial differences in the displacement field and avoids an assumption of the weak differentiability. Hence discontinuities in the displacement field do not lead to an ill-posed system.

A minor simplification of the main result of Du et al. [19] is given by the following result associated with a linear isotropic peridynamic material.

Theorem 6. *Let the nonzero volume $\Omega_c \subset \Omega$ with $\Omega_s \cup \Omega_c = \Omega$ and $\Omega_s \cap \Omega_c = \emptyset$ be given. The volume-constrained problem*

$$\begin{cases} \mathcal{L}(\boldsymbol{u})(\boldsymbol{x}) = \boldsymbol{b}(\boldsymbol{x}), & \boldsymbol{x} \in \Omega_s, \\ \quad \boldsymbol{u}(\boldsymbol{x}) = \boldsymbol{h}_d(\boldsymbol{x}), & \boldsymbol{x} \in \Omega_c, \end{cases} \tag{22}$$

is well-posed on $L^2(\Omega_s)^d$ when $\boldsymbol{b} \in L^2(\Omega_s)^d$, given the volume-constraint $\boldsymbol{h}_d$ and mild conditions on η and γ.

The volume-constraint is the nonlocal analogue of a boundary condition, necessary for the well-posedness of a boundary value problem. The above theorem is established by demonstrating that (22) is the optimality system associated with a quadratic functional with a unique minimizer. Nonlocal analogues of Korn's inequality and Green's identities are needed.

4 Peridynamics as a multiscale method

4.1 Limit of vanishing nonlocality

A fundamental question of the peridynamic theory was if it generalizes the conventional linear elastic theory. More precisely, does the nonlocal linear peridynamic equation of motion converge towards the Navier equation of linear

elasticity? Indeed in [25], Emmrich and Weckner proved convergence in an interior subdomain under smoothness assumptions of the solution. Therefore, let $\Lambda \subset \mathbb{R}^+$ be a null sequence bounded by some $\delta_0 > 0$, Ω_0 be the interior subdomain defined as all $\boldsymbol{x} \in \Omega$ such that $\operatorname{dist}(x, \partial\Omega) > \delta_0$, $L_{d,\delta}$ the linear operator defined through (7) and L the operator corresponding to the Navier equation of linear elasticity defined through (1) (with $\lambda = \mu$ since $\nu = 1/4$).

Theorem 7. *Let (17) be valid for all $\delta \in \Lambda$ and $\lambda_{d,\delta}$ be nonnegative. If $\boldsymbol{v} \in \mathcal{C}^2(\Omega)^d$ then*

$$\|L_{d,\delta}\boldsymbol{v} - L\boldsymbol{v}\|_{L^\infty(\Omega_0)^d} \to 0 \quad \text{as} \quad \delta \to 0 \quad (\delta \in \Lambda).$$

In addition, an expansion of $L_{d,\delta}\boldsymbol{v}$ in terms of a series of differential operators of even order $2n$ ($n = 1, 2, \dots$) applied to $\boldsymbol{v}$ can be shown for smooth $\boldsymbol{v}$, where the second-order differential operator is the Navier operator and where the coefficients of the differential operators behave like $\delta^{2(n-1)}$. This resembles, in the one-dimensional case, the expansion in Arndt & Griebel [7] for the evolution equation of an atomistic system as well as the higher-order Boussinesq equation appearing in the work of Duruk, Erbay & Erkip [22]. A similar observation has also been made in Emmrich & Weckner [24] when discussing the relation between the peridynamic elastic bar and nonlinear dispersion relations: different dispersion relations correspond to different micromodulus functions, which then correspond (for smooth solutions) to different higher-order differential equations.

Furthermore in [21], Du and Zhou have also investigated the limit of vanishing nonlocality in the case of the full space $\Omega = \mathbb{R}^d$ being then able to show convergence of the sequence of solutions.

Theorem 8. *Let (18) be valid and $\lambda_{d,\delta}(r) > 0$ for $0 < r < \delta$. If $\boldsymbol{u}_0 \in H^1(\mathbb{R}^d)^d$, $\dot{\boldsymbol{u}}_0 \in L^2(\mathbb{R}^d)^d$ and $\boldsymbol{b} \in L^2(0,T;L^2(\mathbb{R}^d)^d)$, then the solution of the initial-value problem (7), (4) converges to the solution of the initial-value problem (1), (4) as $\delta \to 0$ in the conventional norms of $L^2(0,T;\mathcal{M}_\lambda(\mathbb{R}^d)^d) \cap H^1(0,T;L^2(\mathbb{R}^d)^d)$ if*

$$\int_{B_\delta(\mathbf{0})} \lambda_{d,\delta}(|\boldsymbol{x}|)\,|\boldsymbol{x}|^4\,d\boldsymbol{x} \to 2d(d+2)\mu \quad \text{as} \quad \delta \to 0.$$

Note that here no extra regularity of the solution is assumed. Recall that if (17) is also fulfilled, then $\mathcal{M}_\lambda(\mathbb{R}^d)^d = L^2(\mathbb{R}^d)^d$ and (18) is always fulfilled if the deformation energy density for isotropic expansion arising from the peridynamic model coincides with the energy density known from the classical linear elasticity theory.

The limit of vanishing nonlocality of the state-based model is investigated in Lehoucq & Silling [45], see also Section 3.4.

4.2 Composite material and two-scale convergence

In [4], Alali and Lipton focus on the modeling and analysis of heterogeneous media using the peridynamic formulation. Considering both macroscopic and microscopic dynamics in one model, the so-called two-scale convergence is essential to approximate a solution.

In detail, a peridynamic long-range force is perturbed by an oscillating short-range force representing the heterogeneities. For example, one can think of a fibre-reinforced composite. The deformations are assumed to be small, this justifies, that both the long scale macroscopic force function f_{long} and the short-scale microscopic force function f_{short} are linearizations of the bond-strech model (see Section 2.2). The connection between those two scales is described by a parameter ε. The displacement inside the composite is denoted by $\boldsymbol{u}_\varepsilon = \boldsymbol{u}_\varepsilon(\boldsymbol{x},t)$. The peridynamic equation of motion for heterogeneous material reads

$$\begin{aligned}\rho_\varepsilon(\boldsymbol{x})\partial_t^2\boldsymbol{u}_\varepsilon(\boldsymbol{x},t) = &\int_{\mathcal{H}_{long}(\boldsymbol{x})} \boldsymbol{f}_{long}(\hat{\boldsymbol{x}}-\boldsymbol{x}, \boldsymbol{u}_\varepsilon(\hat{\boldsymbol{x}},t)-\boldsymbol{u}_\varepsilon(\boldsymbol{x},t))d\hat{\boldsymbol{x}}\\ &+\int_{\mathcal{H}_{short}(\boldsymbol{x})} \boldsymbol{f}_{short}(\boldsymbol{x},\hat{\boldsymbol{x}}-\boldsymbol{x}, \boldsymbol{u}_\varepsilon(\hat{\boldsymbol{x}},t)-\boldsymbol{u}_\varepsilon(\boldsymbol{x},t))d\hat{\boldsymbol{x}}\\ &+\boldsymbol{b}_\varepsilon(\boldsymbol{x},t), \quad (\boldsymbol{x},t)\in\Omega\times(0,T).\end{aligned} \tag{23}$$

Note that the microscopic force function now explicitly depends on $\boldsymbol{x}$ since the bond strength is influenced by the distance of the *fast* parameters of $\boldsymbol{x}/\varepsilon$ and $\hat{\boldsymbol{x}}/\varepsilon$. The macroscopic integration volume $\mathcal{H}_{long}(\boldsymbol{x})$ is the open ball with centre $\boldsymbol{x}$ and radius $\delta_1 > 0$ intersected with Ω, the microscopic integration volume $\mathcal{H}_{short}(\boldsymbol{x})$ is the open ball with centre $\boldsymbol{x}$ and radius $\varepsilon\delta_2 > 0$ intersected with Ω. Alali & Lipton [4] show well-posedness of (23) complemented with initial conditions. Furthermore they show that the displacement $\boldsymbol{u}_\varepsilon = \boldsymbol{u}_\varepsilon(\boldsymbol{x},t)$ can be approximated by a function $\boldsymbol{u} = \boldsymbol{u}(\boldsymbol{x},\boldsymbol{x}/\varepsilon,t)$. Indeed, setting $\boldsymbol{y} = \boldsymbol{x}/\varepsilon$, $\boldsymbol{u} = \boldsymbol{u}(\boldsymbol{x},\boldsymbol{y},t)$ is the two-scale limit of $\boldsymbol{u}_\varepsilon = \boldsymbol{u}_\varepsilon(\boldsymbol{x},t)$, that is

$$\int_{\Omega\times(0,T)} \boldsymbol{u}_\varepsilon(\boldsymbol{x},t)\Psi\left(\boldsymbol{x},\boldsymbol{x}/\varepsilon,t\right)d\boldsymbol{x}dt \to \int_{\Omega\times Y\times(0,T)} \boldsymbol{u}(\boldsymbol{x},\boldsymbol{y},t)\Psi\left(\boldsymbol{x},\boldsymbol{y},t\right)d\boldsymbol{x}d\boldsymbol{y}dt$$

for all $\Psi \in C_c^\infty(\mathbb{R}^3\times Y\times\mathbb{R}^+)$, that are Y-periodic in y, as ε tends to zero. Here $Y\subset\mathbb{R}^3$ is the unit period cube with the origin at the center. The function $\boldsymbol{u} = \boldsymbol{u}(\boldsymbol{x},\boldsymbol{y},t)$ is obtained from a partial integro-differential initial value problem which is similar to (23) but independent of ε.

5 Numerical approximation

In what follows, we only describe the quadrature formula method. For a finite element approximation, we refer to Chen & Gunzburger [14].

Let $\Omega\subset\mathbb{R}^d$ ($d\in\{2,3\}$) be (for simplicity) a polyhedral domain and let $\mathbb{T} = \{\mathcal{T}_\ell\}_{\ell\in\mathbb{N}}$ be a sequence of partitions of Ω such that

(i) $\mathcal{T} = \{T_i\}_{i=1}^M$ for any $\mathcal{T} \in \mathbb{T}$ with T_i ($i = 1, \dots, M$, $M \in \mathbb{N}$) being a closed triangle (tetrahedron) or parallelogram (parallelepiped) with nonempty interior $\mathring{T}_i$ such that

$$\bigcup_{i=1}^{M} T_i = \overline{\Omega}\,,\ \mathring{T}_i \cap \mathring{T}_j = \emptyset \text{ for } i \neq j\ (i, j = 1, \dots, M)\,;$$

(ii) there exist constants $c_1 > 0$ and $c_2 > 0$ such that for all $\mathcal{T} \in \mathbb{T}$ and all $T \in \mathcal{T}$

$$h_{\max} := \max_{T\in\mathcal{T}} h_T \leq c_1 h_T \leq c_2 \rho_{\min} := \min_{T\in\mathcal{T}} \rho_T$$

with $h_T := \operatorname{diam} T$ being the diameter of T and ρ_T being the radius of the largest inscribed ball of T (quasi-uniformity);

(iii) $h_{\max}(\mathcal{T}_\ell) := \max_{T\in\mathcal{T}_\ell} h_T \to 0$ as $\ell \to \infty$.

We now describe the quadrature formula method for the spatial approximation of (7). Let $\phi \in \mathcal{C}(\overline{\Omega})$. On each $T \in \mathcal{T} \in \mathbb{T}$, we consider the quadrature formula

$$Q_T[\phi] := \sum_{\mu=1}^{m_T} \omega_{T,\mu}\phi(\boldsymbol{x}_{T,\mu}) \approx \int_T \phi(\hat{\boldsymbol{x}})d\hat{\boldsymbol{x}} =: I_T[\phi]$$

with the quadrature points $\boldsymbol{x}_{T,\mu} \in T$ (remember that T is closed and quadrature points can also lie on the boundary of T) and weights $\omega_{T,\mu} > 0$ ($\mu = 1, \dots, m_T \in \mathbb{N}$). We then get the composed quadrature formula

$$Q_\Omega[\phi] := \sum_{T\in\mathcal{T}} Q_T[\phi] \approx I_\Omega[\phi]\,.$$

By introducing a global numbering of the quadrature points $\boldsymbol{x}_{T,\mu}$ (each quadrature point is only counted once), we find

$$Q_\Omega[\phi] = \sum_{j=1}^{N} \omega_j \phi(\boldsymbol{x}_j)$$

with globally numbered weights ω_j. Note that ω_j is the sum of all the local weights corresponding to the quadrature point $\boldsymbol{x}_j$. For having a consistent quadrature, certain additional standard assumptions are required, which we are not going to specify here.

Using the quadrature points as collocation points for the approximation of (7), we arrive at

$$\begin{aligned}
&\rho(\boldsymbol{x}_i)\partial_t^2 \boldsymbol{u}_i(t) = (L_{d,\delta}^{(h)}\boldsymbol{u}^{(h)})(\boldsymbol{x}_i, t) + \boldsymbol{b}(\boldsymbol{x}_i, t)\,, \quad i = 1, \dots, N\,,\\
&\text{with } (L_{d,\delta}^{(h)}\boldsymbol{u}^{(h)})(\boldsymbol{x}_i, t)\\
&:= \sum_{j\in J(i)} \omega_j \lambda_{d,\delta}(|\boldsymbol{x}_j - \boldsymbol{x}_i|)(\boldsymbol{x}_j - \boldsymbol{x}_i) \otimes (\boldsymbol{x}_j - \boldsymbol{x}_i)(\boldsymbol{u}_j(t) - \boldsymbol{u}_i(t))
\end{aligned}$$

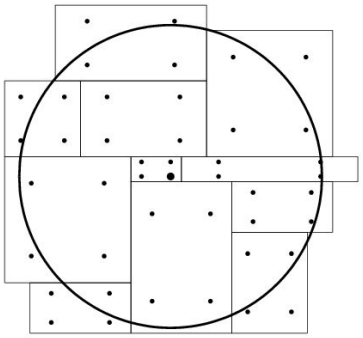

Figure 2. Discretization of the integration volume

and with $\boldsymbol{u}_i(t)$ being an approximation of $\boldsymbol{u}(\boldsymbol{x}_i,t)$ and $\boldsymbol{v}^{(h)}(\boldsymbol{x}_i) := \boldsymbol{v}_i$ for a grid function $\boldsymbol{v}^{(h)}$. Since the integration only takes place in the ball of radius δ intersected with Ω (see also Figure 2), we take

$$J(i) := \{j \in \{1,2,\dots,N\} \setminus \{i\} : |\boldsymbol{x}_j - \boldsymbol{x}_i| < \delta\}\,.$$

As is seen, we take the global weight corresponding to a quadrature point even if not all the elements to which this quadrature point belongs are fully inside the peridynamic horizon. Moreover, if a quadrature point lies on the boundary of the peridynamic horizon than it is not taken into account. One may object that it should be better not to work with the global but with the local weight here. However, this cannot influence the order of approximation.

Let us assume that the displacement field is smooth and that the quadrature rules are exact at least for polynomials of degree $r-1$. Moreover, let us consider the case of the linearization of the bond-based peridynamic model with a suitable regularization in order to avoid the jump discontinuity along the boundary of the peridynamic horizon such as $\lambda_{d,\delta}(r) = \tilde{c}_{d,\delta} r^{-3} \exp(-\delta^2/(\delta^2 - r^2))\chi_{(0,\delta)}(r)$ (see Emmrich & Weckner [25]).

Based upon an estimate of the local error of the quadrature rule, taking into account the growth behaviour of the weak singularity of the integral kernel, and employing stability of the solution with respect to perturbations of the integral kernel, an error estimate of order $\mathcal{O}(h_{\max}^{\min(r,d)})$ and $\mathcal{O}(h_{\max}^{d} \log 1/h)$ if $r = d$, respectively, has been shown in Büsing [13], where d denotes the dimension of the domain. The restriction of the order to the dimension d could not be overcome due to the singularity behaviour of the integral kernel.

6 Applications and numerical simulations

6.1 Simulation of Nanofibres

Investigating the behaviour of nanofibre networks and thin membranes of nanofibres is of great economical and scientific interest. Bobaru [10] and Bobaru, Jiang & Silling [12] have analyzed the behaviour of these fabrics under dynamic deformation including the influence of van der Waals forces. Assuming linear-elastic behaviour on each fibre we have a micropotential as given in Section 2.2. In order to avoid modeling atoms, the van der Waals forces acting between fibres are modeled by adding the so-called Lennard–Jones type potential of the form

$$w^{LJ}(|\boldsymbol{\xi}+\boldsymbol{\eta}|) = \alpha\left(\frac{a}{|\boldsymbol{\xi}+\boldsymbol{\eta}|}\right)^{12} - \beta\left(\frac{a}{|\boldsymbol{\xi}+\boldsymbol{\eta}|}\right)^{6}$$

with parametres α, β and a to the microelastic potential. Since van der Waals forces are long-range forces, the linearized peridynamic equation of motion (7) is complemented with an integral of the Lennard–Jones force density over a horizon which is different to δ.

6.2 Simulation of Cracks

Accurate crack prediction is of topical interest and many authors have worked on it over the last years, see, e.g., Aidun & Silling [3], Agwai, Guven & Madenci [1, 2], Askari, Xu & Silling [8], Bobaru & Ha [11], Huang, Zhang & Qiao [30], and Kilic & Madenci [31]. According to [3], the so-called Kalthoff–Winkler experiment is one of twelve characteristic phenomena of dynamic fracture, which a good numerical simulation should be able to reproduce. In this experiment, a cylindrical steel impactor strikes on the edge of a plate, which has been primed with to parallel notches. If the strike is fast enough, the crack propagates in a characteristic angle (see Figure 3). Silling [42] shows that the Kalthoff–Winkler experiment is correctly simulated with the peridynamic theory. In [3] the simulation of further characteristic phenomena of dynamic fracture with the peridynamic theory is investigated.

Acknowledgment

The authors are grateful to Stephan Kusche and Henrik Büsing for the numerical simulation of the Kalthoff–Winkler experiment.

References

1. A. Agwai, I. Guven, and E. Madenci, *Peridynamic theory for impact damage prediction and propagation in electronic packages due to drop*, Proceedings of the 58th Electronic Components and Technology Conference, 2008, pp. 1048–1053.

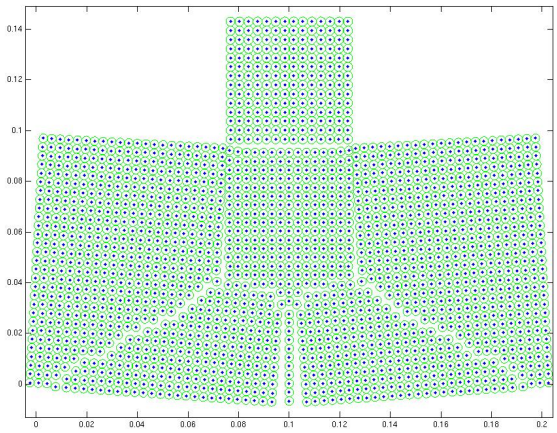

Figure 3. Kalthoff–Winkler experiment

2. _____, *Predicting crack propagation with peridynamics: a comparative study*, Int. J. Fract. **171** (2011), no. 1, 65–78.
3. J. B. Aidun and S. A. Silling, *Accurate prediction of dynamic fracture with peridynamics*, Joint US-Russian Conference on Advances in Materials Science, Prague, 2009.
4. B. Alali and R. Lipton, *Multiscale dynamics of heterogeneous media in the peridynamic formulation*, J. Elasticity **106** (2012), no. 1, 71–103.
5. B. S. Altan, *Uniqueness of initial-boundary value problems in nonlocal elasticity*, Int. J. Solids Structures **25** (1989), no. 11, 1271–1278.
6. _____, *Uniqueness in nonlocal thermoelasticity*, J. Thermal Stresses **14** (1991), 121–128.
7. M. Arndt and M. Griebel, *Derivation of higher order gradient continuum models from atomistic models for crystalline solids*, Multiscale Model. Simul. **4** (2005), no. 2, 531–562.
8. A. Askari, J. Xu, and S. A. Silling, *Peridynamic analysis of damage and failure in composites*, 44th AIAA Aerospace Sciences Meeting and Exhibit (Reno, Nevada), 2006, AIAA-2006-88.
9. Z. P. Bažant and M. Jirásek, *Nonlocal integral formulations of plasticity and damage: survey of progress*, J. Eng. Mech. **128** (2002), no. 11, 1119–1149.
10. F. Bobaru, *Influence of van der Waals forces on increasing the strength and toughness in dynamic fracture of nanofiber networks: a peridynamic approach*, Model. Simul. Mater. Sc. **15** (2007), 397–417.
11. F. Bobaru and Y. D. Ha, *Studies of dynamic crack propagation and crack branching with peridynamics*, Int. J. Fract. **162** (2010), no. 1-2, 229–244.
12. F. Bobaru, H. Jiang, and S. A. Silling, *Peridynamic fracture and damage modeling of membranes and nanofiber networks*, Proc. XI Int. Conf. Fracture, Turin, vol. 5748, 2005, pp. 1–6.
13. H. Büsing, *Multivariate Integration und Anwendungen in der Peridynamik*, Diploma thesis, TU Berlin, Institut für Mathematik, 2008.

14. X. Chen and M. Gunzburger, *Continuous and discontinuous finite element methods for a peridynamics model of mechanics*, Comput. Meth. Appl. Mech. Engin. **200** (2011), no. 9–12, 1237–1250.
15. Y. Chen, J. D. Lee, and A. Eskandarian, *Dynamic meshless method applied to nonlocal crack problems*, Theor. Appl. Fracture Mech. **38** (2002), 293–300.
16. ———, *Atomistic viewpoint of the applicability of microcontinuum theories*, Int. J. Solids Structures **41** (2004), no. 8, 2085–2097.
17. Q. Du, M. Gunzburger, R. B. Lehoucq, and K. Zhou, *A nonlocal vector calculus, nonlocal volume-constrained problems, and nonlocal balance laws*, Technical report 2010-8353J, Sandia National Laboratories, 2010.
18. ———, *Analysis and approximation of nonlocal diffusion problems with volume constraints*, Technical report 2011-3168J, Sandia National Laboratories, 2011, accepted for publication in SIAM Review.
19. ———, *Application of a nonlocal vector calculus to the analysis of linear peridynamic materials*, Technical report 2011-3870J, Sandia National Laboratories, 2011.
20. Q. Du, J. R. Kamm, R. B. Lehoucq, and M. L. Parks, *A new approach for a nonlocal, nonlinear conservation law*, SIAM J. Appl. Math. **72** (2012), no. 1, 464–487.
21. Q. Du and K. Zhou, *Mathematical analysis for the peridynamic nonlocal continuum theory*, M2AN Math. Mod. Numer. Anal. **45** (2011), no. 2, 217–234.
22. N. Duruk, H. A. Erbay, and A. Erkip, *Global existence and blow-up for a class of nonlocal nonlinear Cauchy problems arising in elasticity*, Nonlinearity **23** (2010), 107–118.
23. E. Emmrich and O. Weckner, *The peridynamic equation of motion in non-local elasticity theory*, III European Conference on Computational Mechanics. Solids, Structures and Coupled Problems in Engineering (C. A. Mota Soares et al., ed.), Springer, Lisbon, 2006.
24. E. Emmrich and O. Weckner, *Analysis and numerical approximation of an integro-differential equation modelling non-local effects in linear elasticity*, Math. Mech. Solids. **12** (2007), no. 4, 363–384.
25. E. Emmrich and O. Weckner, *On the well-posedness of the linear peridynamic model and its convergence towards the Navier equation of linear elasticity*, Commun. Math. Sci. **5** (2007), no. 4, 851–864.
26. ———, *The peridynamic equation and its spatial discretisation*, Math. Model. Anal. **12** (2007), no. 1, 17–27.
27. H. A. Erbay, A. Erkip, and G. M. Muslu, *The Cauchy problem for a one dimensional nonlinear elastic peridynamic model*, J. Differential Eqs. **252** (2012), 4392–4409.
28. A. C. Eringen, *Vistas of nonlocal continuum physics*, Int. J. Eng. Sci. **30** (1992), no. 10, 1551–1565.
29. M. Gunzburger and R. B. Lehoucq, *A nonlocal vector calculus with application to nonlocal boundary value problems*, Multscale Model. Simul. **8** (2010), 1581–1598, doi:10.1137/090766607.
30. D. Huang, Q. Zhang, and P. Qiao, *Damage and progressive failure of concrete structures using non-local peridynamic modeling*, Sci. China Tech. Sci. **54** (2011), no. 3, 591–596.
31. B. Kilic and E. Madenci, *Prediction of crack paths in a quenched glass plate by using peridynamic theory*, Int. J. Fract. **156** (2009), no. 2, 165–177.

32. E. Kröner, *Elasticity theory of materials with long range cohesive forces*, Int. J. Solids Structures **3** (1967), 731–742.
33. I. A. Kunin, *Elastic Media with Microstructure, vol. I and II*, Springer, Berlin, 1982/83.
34. R. B. Lehoucq and M. P. Sears, *Statistical mechanical foundation of the peridynamic nonlocal continuum theory: Energy and momentum conservation laws*, Phys. Rev. E **84** (2011), 031112.
35. Y. Lei, M. I. Friswell, and S. Adhikari, *A Galerkin method for distributed systems with non-local damping*, Int. J. Solids Structures **43** (2006), no. 11–12, 3381–3400.
36. A. A. Pisano and P. Fuschi, *Closed form solution for a nonlocal elastic bar in tension*, Int. J. Solids Structures **40** (2003), no. 1, 13–23.
37. C. Polizzotto, *Nonlocal elasticity and related variational principles*, Int. J. Solids Structures **38** (2001), no. 42–43, 7359–7380.
38. ———, *Unified thermodynamic framework for nonlocal/gradient continuum mechanics*, Eur. J. Mech. A/Solids **22** (2003), 651–668.
39. D. Rugola, *Nonlocal Theory of Material Media*, Springer, Berlin, 1982.
40. P. Seleson, M. L. Parks, and M. Gunzburger, *Peridynamic solid mechanics and the embedded atom model*, Technical report SAND2010-8547J, Sandia National Laboratories, 2011.
41. S. A. Silling, *Reformulation of elasticity theory for discontinuities and long-range forces*, J. Mech. Phys. Solids **48** (2000), no. 1, 175–209.
42. ———, *Peridynamic Modeling of the Kalthoff-Winkler Experiment*, Submission for the 2001 Sandia Prize in Computational Science, 2002.
43. S. A. Silling, *Linearized theory of peridynamic states*, J. Elasticity **99** (2010), 85–111.
44. S. A. Silling, M. Epton, O. Weckner, J. Xu, and E. Askari, *Peridynamic states and constitutive modeling*, J. Elasticity **88** (2007), 151–184.
45. S. A. Silling and R. B. Lehoucq, *Convergence of peridynamics to classical elasticity theory*, J. Elasticity **93** (2008), no. 1, 13–37.
46. S. A. Silling and R. B. Lehoucq, *Peridynamic Theory of Solid Mechanics*, Adv. Appl. Mech. **44** (2010), 73–168.
47. J. Wang and R. S. Dhaliwal, *On some theorems in the nonlocal theory of micropolar elasticity*, Int. J. Solids Structures **30** (1993), no. 10, 1331–1338.
48. ———, *Uniqueness in generalized nonlocal thermoelasticity*, J. Thermal Stresses **16** (1993), 71–77.
49. K. Zhou and Q. Du, *Mathematical and numerical analysis of linear peridynamic models with nonlocal boundary conditions*, SIAM J. Numer. Anal. **48** (2010), no. 5, 1759–1780.